

Impact of Synthesis Techniques on the Electrochemical Properties of $ZnCo_2O_4$ as Alternative Anode for Lithium-ion Batteries

Shivangi Rajput^a, Amrish K Panwar^{a*}, & Amit Gupta^b

^aDepartment of Applied Physics, Delhi Technological University, New Delhi 110 042, India

^bDepartment of Mechanical Engineering, IIT Delhi, New Delhi 110 016, India

Received: 9 August 2023; Accepted: 26 September 2023

Nowadays, mixed metal oxides like AB_2O_4 -type structures have gained more and more attention as energy storage materials due to their superior electrochemical performance, better structure stability, good electronic conductivity, and excellent reversible capacity. Herein, $ZnCo_2O_4$ has been synthesized via two different routes of material synthesis such as urea-assisted combustion and ball milling method. The physicochemical characterization has been carried out with the help of XRD, FESEM, and EDX to confirm the phase, morphology, and elemental composition, respectively. The average crystallite size of $ZnCo_2O_4$ via urea-assisted combustion (ZCU) and the ball milled (ZCB) has been observed to be 57 nm and 70 nm as estimated from XRD. The average particle of $ZnCo_2O_4$ via urea combustion and the ball mill is 20 μm and 49 μm , respectively, as observed by FESEM. The influence of the synthesis route on the electrochemical properties was analyzed via Electrochemical Impedance Spectroscopy and Cyclic Voltammetry.

Keywords: Anode, Electrochemical property, Mixed metal oxides, Urea combustion method

1 Introduction

In the recent past, alternative anode materials for energy devices and energy storage systems have been intensively investigated to overcome the low energy density problem of existing batteries to meet the new age demand for modern electronics and electric vehicles.¹ In a Lithium-ion battery, the anode plays a vital role in accommodating and releasing Lithium ions, which requires a reversible reaction of Li-ion with anode material.²⁻³ Commercial LIBs have used graphitic anode, however, on large-scale production, this anode has struggled with challenges due to their low theoretical specific capacities (372 mAh/g), poor rate performance, and low intercalation potential. Therefore, there has been a need to explore alternative anodes with high energy and power density, low cost, and longer durability. Among the various explored anode materials, Transition metal oxides (TMOs) like ZnO, NiO, Fe_2O_3 , Co_3O_4 , and many more have been rigorously studied in recent years owing to their high theoretical capacity and cycle life.⁴ In the recent past, Co-based anodes have been thoroughly explored in an attempt to replace graphitic anodes. Co_3O_4 has gained much attention due to its high capacity and great cyclic life. However, during 1st discharge cycle, Co_3O_4 suffers irreversible capacity loss and capacity

fading in the charge-discharge process due to volume expansion and contraction. To overcome this problem associated with Co_3O_4 , one way is to replace a metal ion with some other metal ion that can react with Lithium by means of alloying and de-alloying process.⁵ One such metal ion is Zn^{2+} , which can partially substitute Co with the formulation of $ZnCo_2O_4$, maintaining the spinel structure and thus delivering better electrochemical properties. Therefore, $ZnCo_2O_4$ is an alternative anode material with a high theoretical capacity of ~ 975 mAh/g, environmental benignity, and good recyclability as compared to Co_3O_4 .⁶ It is well known that the synthesis route and morphology have a direct effect on the electrochemical performance.

In the present study, $ZnCo_2O_4$ has been synthesized via two different synthesis routes viz. solid-state high-energy ball milling (ZCB) and urea-assisted combustion (ZCU). The effect of the synthesis method on the Physical and electrochemical performance has been analyzed.

2 Materials and Methods

2.1 Synthesis

All the precursors used in the synthesis of $ZnCo_2O_4$ are of laboratory grade made by Sigma Aldrich. In high energy ball milling method, Co $(CH_3COO)_2$ and Zn $(CH_3COO)_2$ were weighed in the

*Corresponding author (E-mail: amrish.phy@dtu.ac.in)

molar ratio 1:2 and added to the ball mill, $C_6H_8O_7$ (120% mole fraction) was used as a chelating agent along with a little amount of de-ionized water. The effective ball milling time was 12 h at an rpm of 300 to obtain the as-prepared sample. The sample was kept in a vacuum oven to dry out the moisture, and a pink colour as-prepared sample was collected. The sample was further treated at 800°C in a muffle furnace to finally obtain ZCB.⁷ In the case of the Urea-assisted combustion method, Sigma Aldrich make $Zn(NO_3)_2 \cdot 6H_2O$ and $Co(NO_3)_2 \cdot 6H_2O$ in the ratio were calculated using a stoichiometric ratio 1:2 and were added in the de-ionized water and mixed under continuous stirring at room temperature. Then, both solutions were mixed together in the aqueous solution of Urea, NH_2CONH_2 (Sigma-Aldrich, >99%). The ratio between metal nitrates and urea was kept at 10:6 for controlled combustion. The obtained final solution was kept under vigorous stirring at 80°C for 30 minutes and after that, the temperature was slowly increased to 300°C to remove excess D.I. During the stirring process, the homogenously mixed solution turned viscous, forming a gel. The viscous gel then foamed and eventually burned on its own at 300°C . The as-prepared sample was collected and calcinated in a furnace at 700°C for 5 hours.⁸ The schematic diagram for the Ball Mill synthesis route and Urea-assisted combustion synthesis route is shown in Fig. 1.

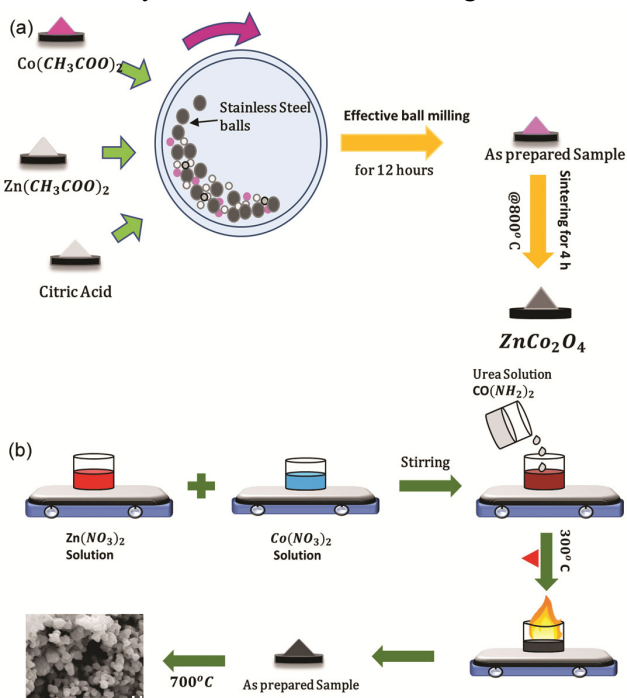


Fig. 1 — Schematic diagram for (a) High energy ball milling route, & (b) Urea combustion route.

2.2 Material and Electrochemical Characterization

Thermogravimetric Analysis (TGA) was investigated using PERKIN ELMER (Model: TGA 4000) at a heating rate of $10^\circ\text{C}/\text{min}$ in air. The crystal structure and phase composition were identified using RIGAKU ULTIMA X-ray Diffractometer equipped with $CuK\alpha 1$ radiation ($\lambda = 1.54 \text{ \AA}$). The XRD pattern was recorded between a range of 10° to 70° (step size = 0.01°). Hitachi S-3700 scanning electron microscope was used to investigate the morphologies. The electrochemical studies were done using CR2016 half cells, keeping the prepared material as an active electrode, the Li chip as a counter electrode, and the polypropylene sheet Celgard 2400 as a separator. For the slurry, 70% of active material, 15% of Acetylene black, and 15% of PVDF in N-methyl-2-pyrrolidone (NMP) was mixed and stirred in a 5 ml beaker @ 50°C for 8 hours. The obtained slurry was then spread onto a Copper foil using Gelon make automatic coating unit followed by drying overnight in a vacuum oven at 100°C . The electrodes of 16 mm diameter were cut and then calendared using the Gelon make rolling press machine to improve the adhesion between the electrode and the Copper foil. The half cell (CR2016) assembly was done in an Ar-filled Mbraun make Glove Box workstation. For the electrolyte, ethylene Carbonate (EC) and Dimethyl Carbonate (DMC) were used in the volume ratio 1:1 to obtain 1 molar solution of $LiPF_6$.

3 Results and Discussion

3.1 Material Characterization

Figure 2 shows the TGA curves of as-synthesized ZCB and ZCU. TGA is used to determine the decomposition of mass w.r.t temperature and hence the reaction route of the precursors. From Fig. 2, it can be seen that both ZCB and ZCU show similar nature of mass decomposition. For both ZCB and ZCU mass loss has been recorded in three steps, it is observed that there is a very small mass loss of $\sim 5.7\%$ from 200°C to 245°C for ZCB and $\sim 3.5\%$ from 190°C to 230°C corresponding to the moisture absorbed in the sample. From 245°C to 350°C , there is a mass loss of 45% for ZCB, and loss of $\sim 47\%$ is observed for ZCU from 230°C to 360°C temperature resulting from the oxidation of residual carbon present in the sample, the sudden loss of 56% for ZCB is observed during 350°C to 750°C , and for ZCU from 360°C to 650°C mass loss of 50% can be ascribed to the decomposition of metal salts present in the

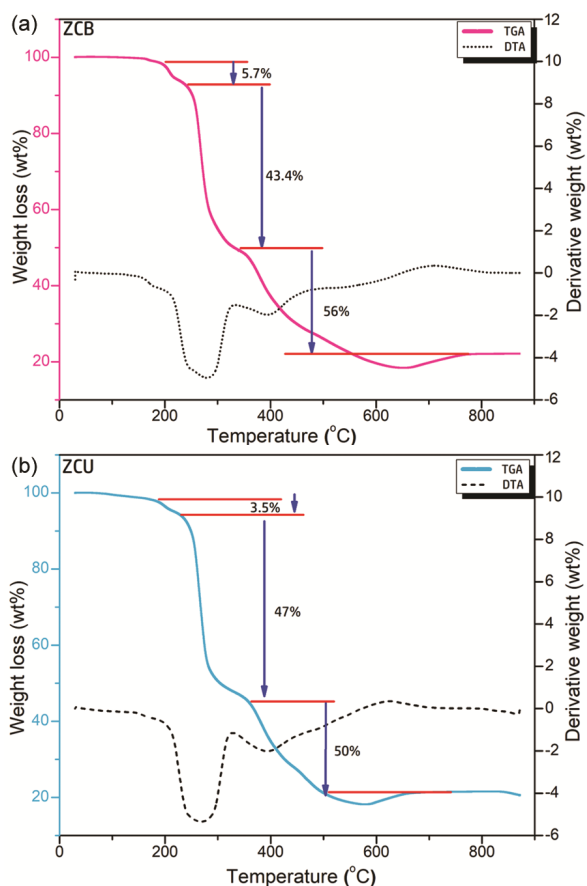


Fig. 2 — TGA curve of as-synthesized (a) ZCB, & (b) ZCU from 30°C to 900 °C.

precursors. After 750 °C for ZCB and after 650 °C for ZCU the mass decomposition stabilizes, which confirms that there is no mass loss, suggesting the desired temperature for the phase formation of $ZnCo_2O_4$.⁹ The XRD patterns for both the synthesized ZCB and ZCU are illustrated in Fig 3(a-b). All the observed peaks match well with the JCPDS card no. 01-081-2296 belonging to the spinel $ZnCo_2O_4$ structure. (111), (220), (311), (222), (400), (422), (511), and (440) are typical reflection planes of XRD patterns of $ZnCo_2O_4$. No traces of impurity are present indicating crystallinity and purity of synthesized ZCB and ZCU. Although some missing peaks and some noise can be detected in the ZCB XRD pattern which could be due to the route opted for synthesis. Scherrer’s formula ($D = k\lambda/\beta \cos\theta$) was used to estimate the crystallite size, where D , λ (0.154 nm), k (0.9), β , and θ denotes the crystallite size, wavelength of X-ray radiation, Scherrer’s constant, FWHM, and diffraction angle, respectively. The crystallite size as estimated from Scherrer’s formula is 70 nm and 57 nm for ZCB and ZCU, respectively.¹⁰⁻¹¹

The morphologies of the synthesized ZCB and ZCU are shown in Fig. 3(c-d). As Displayed in Fig. 3(c), ZCB shows non-uniform agglomerated microstructures with an average size of 49 μm whereas, ZCU demonstrates nearly spherical shaped with less agglomerated particles with an average size

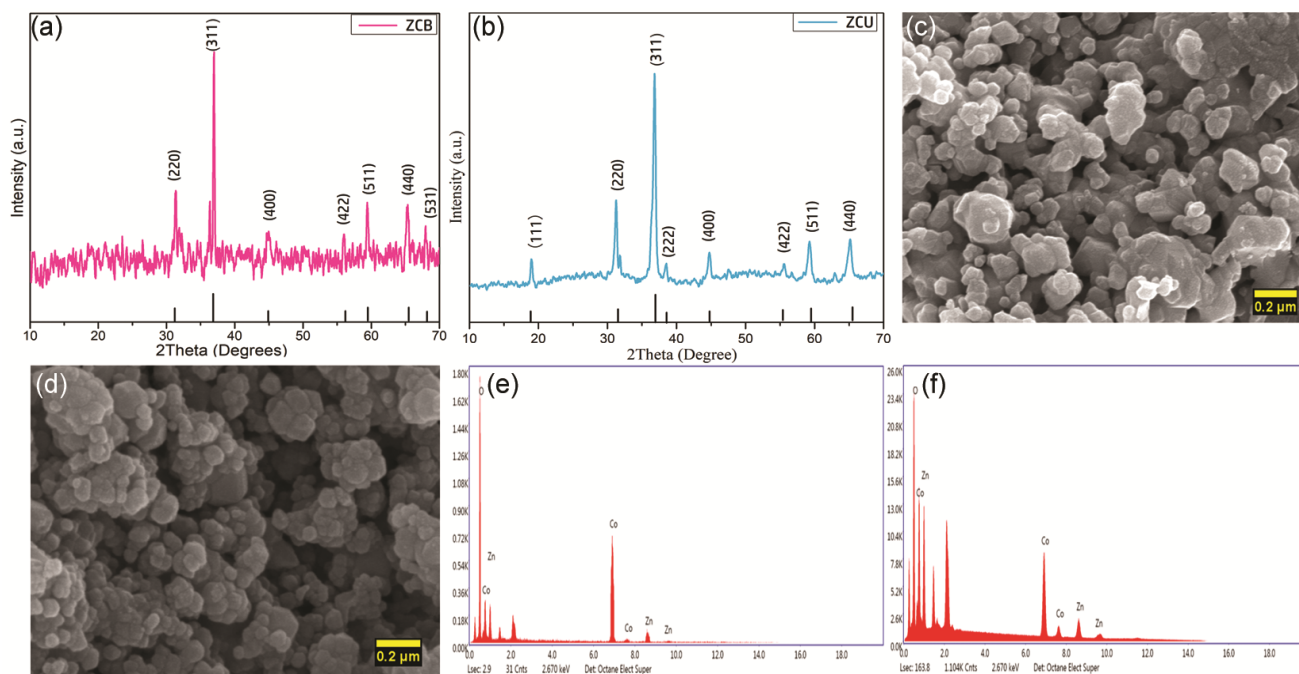


Fig. 3 — XRD pattern recorded from 10-90° (a) ZCB, (b) ZCU, SEM micrographs for, (c) ZCB, (d) ZCU, EDX spectrum for, (e) ZCB, (f) ZCU.

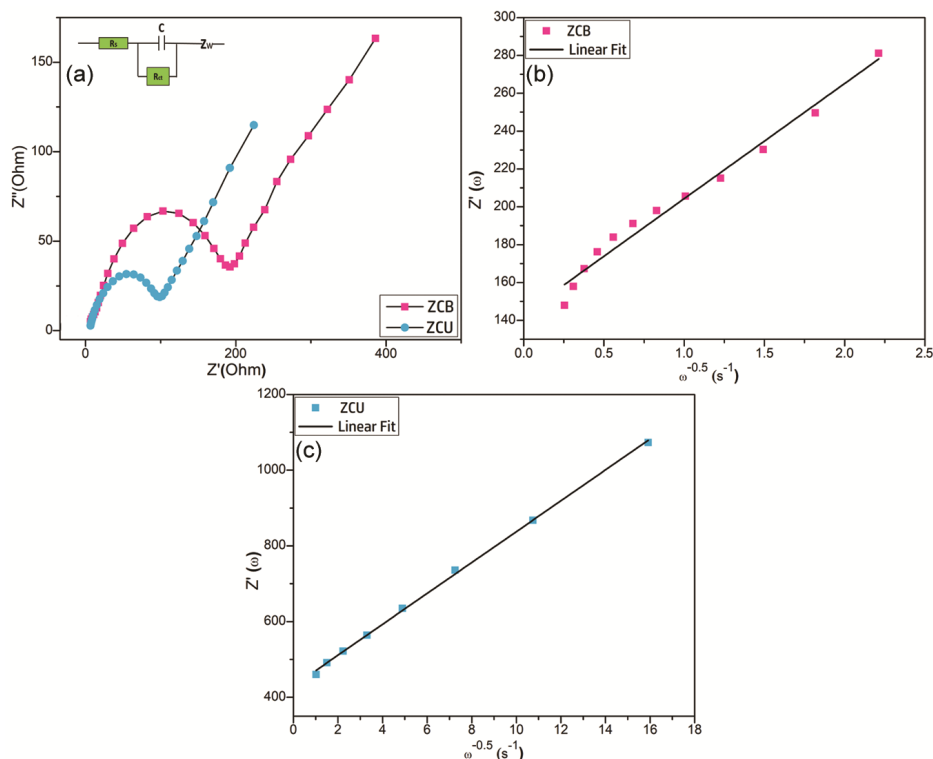


Fig. 4 — (a) Nyquist plots of the ZCB and ZCU recorded in the frequency range 10 mHz-10 KHz, the relationship between real Z and square root inverse of ω for, (b) ZCB, & (c) ZCU.

Table 1 — EIS Analysis of ZCB and ZCU electrodes recorded from 10KHz to 10mHz with the AC amplitude of 5mV

	R_s (Ω)	R_{ct} (Ω)	σ_ω ($\Omega s^{-1/2}$)	D_{Li^+} ($cm^2 s^{-1}$)
ZCB	5.69	207	60.56	9.32×10^{-15}
ZCU	5.58	110	40.78	2.63×10^{-14}

of 20 μ m. The EDX spectra are shown in Fig 3(e-f) and it can be seen that the prepared samples ZCB and ZCU consist of elements Zn, Co, and O only and there is no impurity present in the samples.

3.2 Electrochemical Characterization

Electrochemical Impedance Spectroscopy (EIS) was done at OCV to understand the kinetic behavior of ZCB and ZCU occurring at the electrode-electrolyte interface. EIS is used to examine the internal impedance of a cell, which has a significant effect on the electrochemical properties. Figure 4(a) shows the EIS curves of ZCB and ZCU at Open Circuit Voltage. As seen from the graphs, both EIS curves show a semicircle at a higher frequency and an inclined straight line at a low frequency. To analyze the EIS results, the fitting of the Nyquist plot has been done using an equivalent circuit. Inset of Fig. 4(a) shows the equivalent circuit, where R_s , R_{ct} , C , and Z_w represent the resistance occurring due to the electrolyte, the resistance due to the interface of

electrode and electrolyte, double layer capacitance, and Warburg impedance, respectively. From Fig 4(a), it can be seen that ZCU has a small diameter of the semicircle than ZCB, indicating that the R_{ct} value is lower for ZCU which implies that the kinetic behavior of ZCU is better than ZCB. Figure 4(b-c) show the graph between Real Z and square root inverse of ω (Bode plot). The diffusion coefficient for the prepared samples was calculated using the following equation:

$$D_{Li^+} = \frac{0.5R^2T^2}{A^2n^2F^2C^2\sigma_\omega^2} \quad \dots(1)$$

Where D_{Li^+} , T , R , n , A , C , F and σ_ω represents Lithium diffusion coefficient ($cm^2 s^{-1}$), Temperature (K), Boltzmann Constant ($8.314, J mol^{-1} K^{-1}$), no. of electrons, Area of electrode (cm^2), concentration of Li-ion (mol / cm^3), Faraday's constant ($\Omega s^{-1/2}$) and Warburg factor. Slope of Bode plot gives Warburg Factor.¹² The calculated values of R_s , R_{ct} , σ_ω and D_{Li^+} are given in Table 1. Cyclic

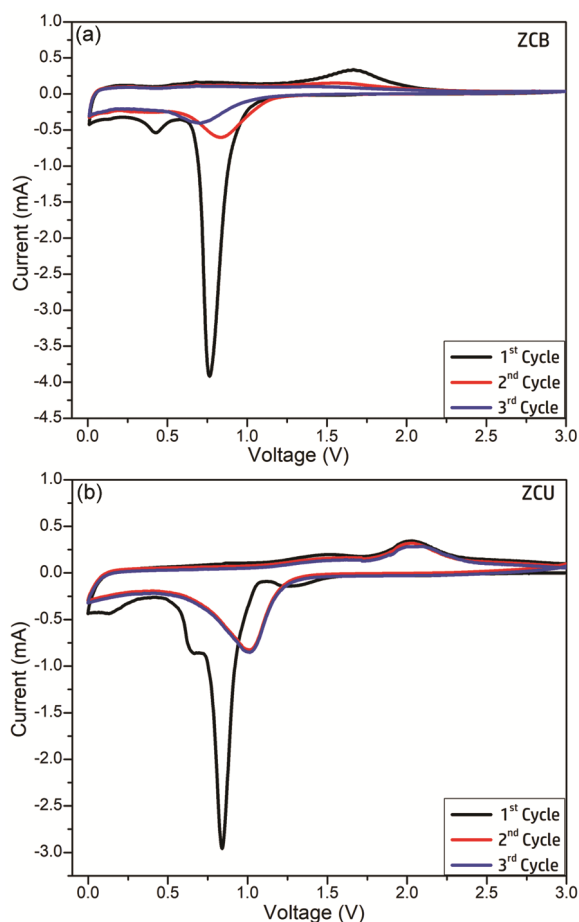
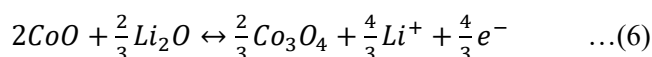
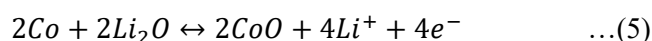
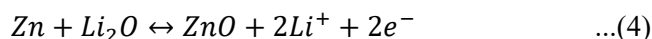
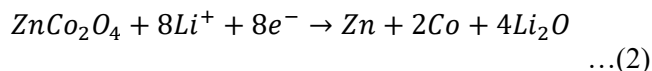


Fig. 5 — CV curves of (a) ZCB, (b) ZCU recorded within the potential window (0.01-3.0V) at 0.05 mV/s scan rate.

Voltammetry study of ZCB and ZCU was investigated at 0.05 mV/s scan rate in the voltage window 0.01 to 3.0 V for the first 3 cycles as shown in Fig. 5(a-b). For ZCB, there is an initial cathodic process observed at 0.77 V and a peak occurring at ~ 0.42 V which could be attributed to the reduction of Zn^{2+} and Co^{3+} to Zn^0 and Co^0 . This peak then further shifts to 1.01 V for 2nd and 3rd Cycle. In the anodic sweep, strong oxidation peak is present at 2.0 V resulting from the oxidation process of Zn and Co to Zn^{2+} and Co^{3+} , which then further vanishes in 2nd and 3rd cycle. For ZCU, the initial cathodic process is observed at 0.83 V and another small peak occurs at ~ 0.66 V which could be assigned to the reduction of $ZnCo_2O_4$ to the metallic Zn^0 and Co^0 . This cathodic peak further shifts to 1.01 V for 2nd and 3rd Cycles. For the anodic sweep, two main peaks are observed at 1.46 and 2.0 V characteristic of the oxidation process of Zn and Co to ZnO and CoO_x . The repeatability of CV graphs are good in ZCU whereas ZCB shows

no repeatability implying the better redox activity of ZCU than ZCB.¹³ The charge discharge electrochemical reactions can be obtained as follows:



4 Conclusion

Two different synthesis routes have been presented: High energy ball mill and Urea-assisted combustion method. The physical and electrochemical properties have been studied and compared using different characterizations. By comparing these two different synthesis route it has been observed that the material synthesized via urea combustion techniques (ZCU) has shown better physical and electrochemical properties than the ball milling route (ZCB). The average size of particles obtained from urea-assisted combustion and ball milled sample has been found to be 29 μm and 40 μm , respectively. The diffusion coefficient calculated from EIS analysis for ZCB and ZCU has been estimated to be $9.32 \times 10^{-15} cm^2 s^{-1}$ and $2.63 \times 10^{-14} cm^2 s^{-1}$, respectively. The cyclic voltammograms of both the prepared electrodes reveal that the cyclability and repeatability of ZCU is better than ZCB, which further suggest that the insertion and extraction of Li-ions is better for ZCU.

Acknowledgement

The Authors are grateful to Delhi Technological University for support and financial assistance through Project grant No. DTU/IRD/619/2019/2114.

References

1. an Y, Zeng W, Li L, Zhang Y, Zong Y, Cao D, Wang G, Lucht B L, Ye K & Cheng K, *Nano-Micro Lett*, 9 (2017)20.
2. Ratha S & Rout C S, *RSC Adv*, 5(2015)86551.
3. Yang Y, Li Z, Xu S, Tang Y Lee C S & Zhang W, *Material Today Energy*, 12(2019) 46.
4. Shih G H & Liu W R, *RSC Adv*, 7 (2017) 42476.
5. Wang L, Li D, Zhang J, Song C Xin H & Qin X, *Ionics*, 26 (2020)4479.
6. Zhang L & Zhu S, *Mat. Letters*, 236 (2019) 337.
7. Wang W, Yang Y, Yang S, Guo Z & Feng C, *Electrochim Acta*, 155 (2015) 297.

- 8 Rai A K, Thi T V, Paul B J & Kim J, *Electrochim Acta*, 146 (2014) 577.
- 9 Venkatachalam V, Alsalmeh A, Alghamdi A & Jayavel R, *Ionics*, 23 (2017)977.
- 10 Xu H, Zhang Y, Song X, Kong X, Ma T & Wang H, *J Alloys Compd*, 821 (2020) 153289.
- 11 Ren H, Wang W, Joo S W, Sun Y &Gu C, *Mater Res Bulletin*, 111 (2019) 34.
- 12 Rajput S, Panwar A K & Gupta A, *Solid state ionics*, 394 (2023) 116206.
- 13 Hou X, Bai S, Xue S, Shang X, Fu Y &He D, *J Alloys Compd*, 711 (2017) 59259.